Available online at www.sciencedirect.com

SciVerse ScienceDirect

Ceramics International 39 (2013) S517–S520

CERAMICS INTERNATIONAL

www.elsevier.com/locate/ceramint

The effects of solvents on the formation of $Ba_{0.65}Sr_{0.35}TiO_3$ thin films derived by sol–gel processing

Xiaoyang Chen[a], Yunfei Tian[b], Hong Liu[a], Cenghu Du[a], Jun Li[a], Ping Yu[a,*]

[a]College of Materials Science and Engineering, Sichuan University, Chengdu, 610064, China
[b]Analytical and Testing Center, Sichuan University, Chengdu 610064, China

Available online 27 October 2012

Abstract

The sol–gel method was used to synthesize $Ba_{0.65}Sr_{0.35}TiO_3$ thin films. Two synthesis routes with two different solvents, ethylene glycol methyl ether and methyl ethyl glycol, were used and compared. $Ba_{0.65}Sr_{0.35}TiO_3$ thin films were deposited on Si substrates by using spin coating technique. The as-deposited dry films were treated with rapid thermal annealing. The effects of solvents on the grain size, morphology, surface roughness, and the phase formation of the $Ba_{0.65}Sr_{0.35}TiO_3$ thin films were studied. Investigation of these films shows that the microstructures of $Ba_{0.65}Sr_{0.35}TiO_3$ thin films prepared from sols using methyl ethyl glycol were more homogeneous and denser; the root mean square (RMS) of the film can reach ~3 nm when annealed at 750 °C.

Keywords: A. Sol–gel process; A. Films; B. Surface; $Ba_{0.65}Sr_{0.35}TiO_3$

1. Introduction

$Ba_{1-x}Sr_xTiO_3$ thin films have been extensively investigated for their emerging applications in the fields of high density DRAM, microwave phase shifters, IR sensing devices, humidity and gas sensors. Different techniques have been employed to prepare $Ba_{1-x}Sr_xTiO_3$ thin films. Among them, the chemical sol–gel synthesis and spin coating is a very versatile technique, which offers much greater flexibility in terms of large area deposition, substrates with non-planer shapes [1], a high degree of homogeneity and incorporation of doping elements. It is well-known that a high defect-state density and surface roughness of thin films can significantly decrease the performance of devices. The research for high quality $Ba_{1-x}Sr_xTiO_3$ thin films has been driven by the numerous demanding for microelectronic devices. The critical problem for BST films derived by sol–gel technology is how to obtain very dense, smooth and crack-free films. A lot of researches have been done to improve the quality of $Ba_{1-x}Sr_xTiO_3$ thin films deposited by sol–gel technique [2–6]. Based on previous experiments, we find that the solvent has an important contribution to the microstructural development and the final dielectric properties of the thin film. However, only a few works report the influence of solvents on the $Ba_{1-x}Sr_xTiO_3$ thin films by using the sol–gel method.

In this work, we focus on the effects of the solvents on the $Ba_{0.65}Sr_{0.35}TiO_3$ (BST) films. Two kinds of solvent are used to synthesis BST precursor sol. This work reports how the solvents affect the particle size, the morphology of crystalline and amorphous–crystalline transition of the BST thin films on molecular scale. The results indicate that the solvent play an integral role in preparation high quality BST thin films.

2. Experimental

$Ba(OOCCH_3)_2 \cdot H_2O$, $Sr(OOCCH_3)_2 \cdot H_2O$ and $Ti(C_4H_9O)_4$ were used as starting materials. In order to understand the influence of solvent on the preparation of $Ba_{0.65}Sr_{0.35}TiO_3$ thin films, two kinds of solvents such as ethylene glycol methyl ether (EGME, 2-methoxyethanol) and methyl ethyl glycol (MEG, Propylene glycol) were used. $Ba(OOCCH_3)_2 \cdot H_2O$ and $Sr(OOCCH_3)_2 \cdot H_2O$ were mixed in a mole ratio of 13:7, and then dissolved in the co-solvents of EGME and acetic acid with a volume ratio of 2:1 and the co-solvents of MEG and acetic acid with a

*Corresponding author. Tel.: +86 28 85412415; fax: +86 28 85452721.
E-mail address: pingyu@scu.edu.cn (P. Yu).

0272-8842/$ - see front matter © 2012 Elsevier Ltd and Techna Group S.r.l. All rights reserved.
http://dx.doi.org/10.1016/j.ceramint.2012.10.125

volume ratio of 2:1 at 120 °C to obtain transparent solutions, respectively. Ti $(C_4H_9O)_4$ was dissolved in EGME and MEG. The dissolved barium and strontium precursor solution was then dropped into Ti $(C_4H_9O)_4$ precursor solution with the same solvent to get the $Ba_{0.65}Sr_{0.35}TiO_3$ (BST) precursor sols. Both the final sols were prepared with the concentration of 0.05 M and 0.2 M, respectively. The $Ba_{0.65}Sr_{0.35}TiO_3$ thin films were fabricated with the following procedure: the sol is spin-coated onto different substrates, single crystal silicon and Pt, at a speed of 4500 rev/min and then dried at 180 °C for several minutes. The deposited thin films were annealed by a rapid thermal annealing (RTA) process at 550 °C, 650 °C, 750 °C for 3 min. The films with desired thickness were obtained by repeating the spinning–heating cycles. Finally, the deposited films were annealed by a conventional thermal annealing (CTA) at 750 °C for 90 min in air.

The crystal phase of BST thin films synthesized in different solvents was determined by using X ray-diffraction (DX-1000, Dandong, China) with Cu Kα radiation ($\lambda = 0.15406$). Thermal analysis (TG) and differential scanning calorimetry (DSC) (Mettler Toledo DSC 822e) were used to determine the pre-heating temperature of the thin films. The surface morphology of the films was analyzed by atomic force microscope (SPA-300HV, Seiko Instruments, Japan).

3. Results and discussion

3.1. Influence of solvents on the synthesis of $Ba_{0.65}Sr_{0.35}TiO_3$

The stability and the gelation time of the as-prepared BST precursor sols were investigated by recording the gelation time of the BST precursor sols at different temperature. As shown in Table 1, the BST–MEG sols maintain clear and transparent for a longer time than the BST–EGME sols. The results show that the gelation time is significantly affected by solvents. The BST–MEG sols exhibit a better time stability.

Table 1
The characteristics of the BST precursor sols[a].

Solvent type	pH value	Viscosity (mPa s)	Gelation time[a] (day)	Gelation time[b] (day)	Gelation time[c] (day)
MEG sol[d]	3.5	66.8	35	21	–
MEG sol[e]	3.8	75.6	15	10	3.5
EGME sol[d]	4.3	1.49	17.5	12	–
EGME sol[e]	4.7	1.60	7	5	1.5

[a] 10 °C.
[b] 20 °C.
[c] 50 °C.
[d] 0.05 M.
[e] 0.2 M.

Previous studies demonstrated that the stability and the gelation time of sols were mainly determined by the solute reaction rate of the hydrolysis and condensation in the solvent [7]. It is well known that $Ti(OC_4H_9)_4$ has a strong tendency to hydrolyze and condense in solution. This can easily leads to a dramatic growth of condensates, such as [–Ti–O–]n in three dimensions until a complete gelation occurs. Usually, the acetic acid is introduced to suppress growth of condensates. In our case, the shorter gelation time of the BST–EGME sols results from the reaction between EGME and acetic acid. As a result of the reaction, partial acetic acid in the solution turned into an ester, resulting in a faster rate of hydrolysis and condensation of $Ti(OC_4H_9)_4$ in BST–EGME sols. This was also revealed by the pH value of the sols. In Table 1, the pH of BST-MEG sol is lower than that of BST–EGME sol. On the other hand, the results of the viscosities of the sols indicate a different rheological behavior between the BST–EGME sols and the BST–MEG sol. The viscosity (1.46 mPa s) of the BST–EGME sol is lower than that (62.3 mPa s) of the BST–MEG sol at 0.05 M concentration.

Fig. 1 illustrates the thermal decomposition behavior of the BST–MEG xerogel. TGA and DSC analyses were carried out in air at a heating rate of 10 °C/min. With increasing temperature, a significant weight loss is observed below 200 °C due to the evaporation of residual solvent in the xerogel. Then, four exothermic peaks at 312 °C, 424 °C, 456 °C and 484 °C appear in the DSC curve, which corresponding to the decomposition of carboxylate–alkoxide precursors [8]. A flat region is then followed in the TG up to 500 °C. Upon further increasing temperature, a step is found in the TG curve ranging from 660 °C to 850 °C, accompanied by an exothermic peak in the DSC curve. This suggests the transformation of intermediate phase $(Ba_{1-x}Sr_x)TiO_2CO_3$ to perovskite phase $Ba_{1-x}Sr_xTiO_3$ [9,10].

The decomposition behavior of the BST–MEG xerogel looks almost similar to that of the BST–EGME xerogel (see Fig. 2). However, the flat region after the decomposition of carboxylate–alkoxide precursor started from 400 °C rather than 500 °C in the case of the BST–MEG xerogel.

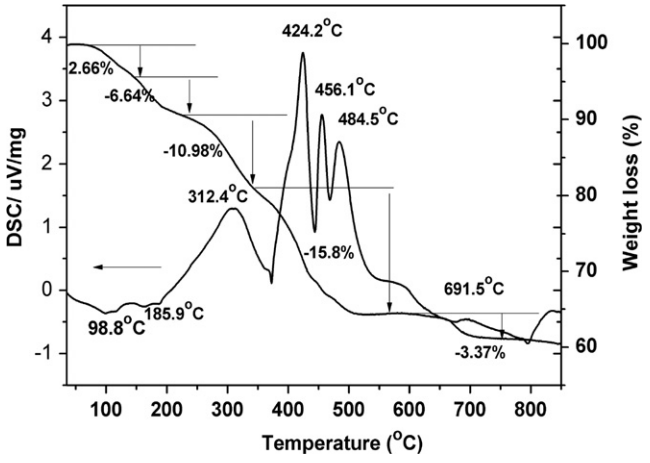

Fig. 1. TG/DSC analyses of the xerogel: precursors prepared in MEG.

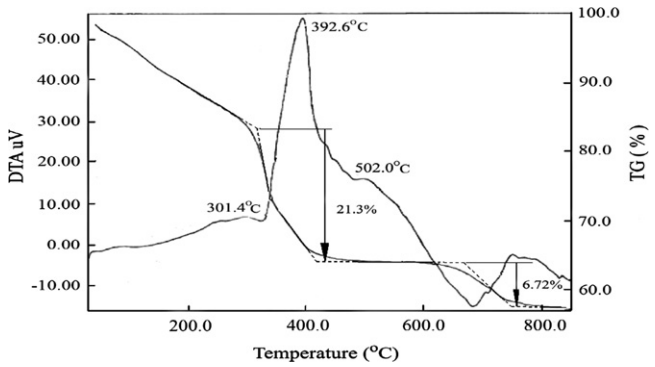

Fig. 2. TG/DTA analyses of the xerogel: precursors prepared in EGME.

In addition, there is a sharp decrease in the weight loss curve within the temperature range from 300 °C to 400 °C, which reveals a faster speed of carboxylate–alkoxide precursor decomposition happened in BST–EGME xerogel.

3.2. Microstructure of the thin films

The XRD patterns of the BST films prepared with two different solvents are shown in Fig. 3. The perovskite phase was clearly formed in the two kinds of thin films after annealed above 650 °C, meanwhile, a small amount of intermediate phase was detected in both the thin films. The secondary phase disappeared and a pure perovskite structure was obtained when the annealing temperature was increased to 750 °C.

It is well known that several factors play important roles in the thin film preparation by sol–gel technique [6,9,11]. One of them is to determine the pre-heating temperature of the thin film after the deposition. During the pre-heating of the thin films, the evaporation of gelation and solvent need some attention. If the gelation occurs more rapidly than the solvent evaporation, the solvent tends to entrap in the gel network, which causes the formation of porous microstructures during annealing. In contrast, if the volatilization of the solvent happens more rapidly than the gelation, the decomposition of the gel induces stress that leads to the peeling of the thin film from the substrate.

In this study, the most active stage of decomposition starts at a lower temperature (180 °C). It is known that thermally induced processes in thin films occur at lower temperatures with regard to the xerogel due to a smaller sample size [12]. By considering the thermal decomposition behavior of the BST–MEG xerogel and the BST–EGME xerogel, the preheating temperature for the preparation of BST thin films was determined to be 180 °C. Using a preheating temperature above 180 °C will lead to the peeling of the BST thin film from the substrate.

Fig. 4 shows the AFM images of the BST films prepared from different precursors with concentrations of 0.05 M and annealed at 750 °C by a RTA process. It can be seen that the thin films made from the BST–MEG sol exhibit a better properties: the surface is denser and more homogeneous. The particle size is about 30 nm and the RMS

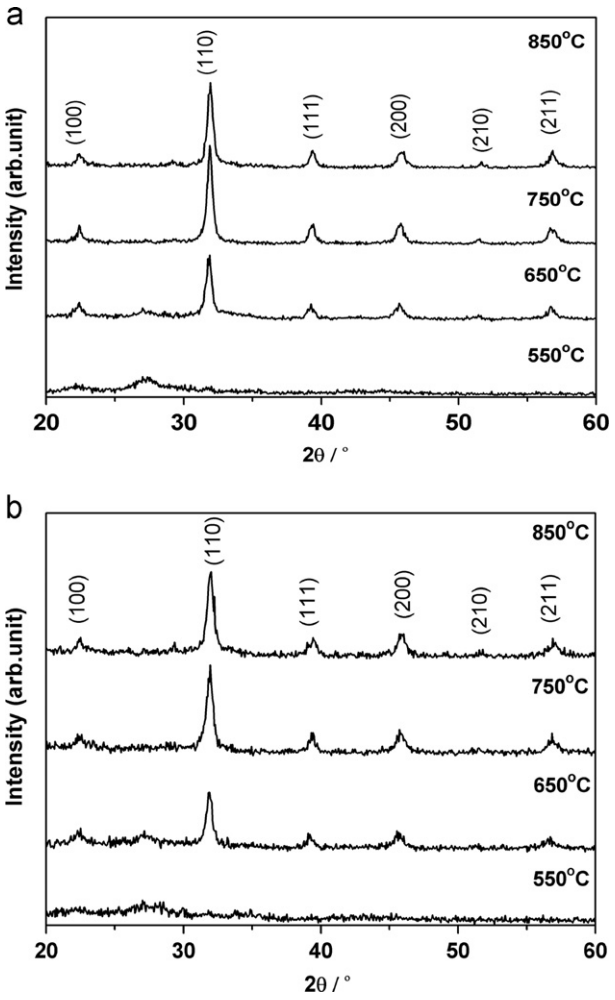

Fig. 3. XRD patterns of the BST films annealed at different temperature prepared in: (a) EGME, and (b) MEG.

(root mean square) of the thin film is 3.562 nm. On the other hand, the films deposited from the BST–EGME sol (Fig. 4b) show a non-uniform microstructure with a grain size of ~50 nm. The RMS value of the thin film is 6.484 nm. The roughness measured by AFM ranged from 60 to 500 nm for the thin films prepared from the BST–EGME sol, whereas the roughness of the thin films prepared from the BST–MEG sol was 30 nm.

The microstructure of the thin films deposited from the BST–EGME sol indicates that the thin film becomes a gel before it dries. This means that a lot of solvent was trapped in the thin film during the evaporation and the heat-treatment processes, which resulted in a high porosity.

4. Conclusions

BST thin films were deposited from different sols and annealed at 750 °C. We observed that the co-solvent had a significant influence on the stability of the sols and the quality of the BST thin films. The study of the stability and the gelation time of the as-prepared BST precursor sols concludes that the hydrolysis and condensation reactions

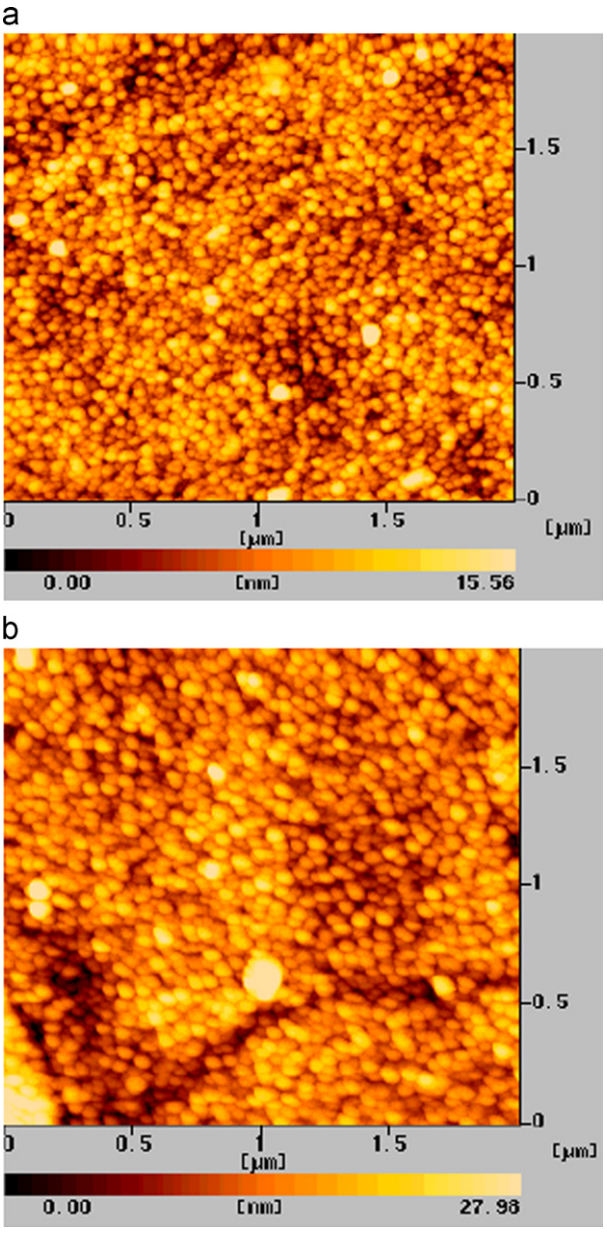

Fig. 4. Atomic force micrographs (AFM) of films annealed at 750 °C prepared in MEG (a) and EGME (b) with concentrations of 0.05 M by a RT process.

are more pronounced in the BST–EMGE sol, which results in a shorter gelation time (c=0.05 M, t_G=12 d) compared to the BST–MEG sol (c=0.05 M, t_G=21 d). The reaction between the EGME and the acetic acid leads to the reduction of the acetic acid, which induces the hydrolysis and condensation of $Ti(OC_4H_9)_4$ in BST–EGME sols. We found that a similar pre-heating temperature of 180 °C can be used for the deposition of BST thin films from the BST–MEG sol and BST–EGME sols. The deposition of the BST thin films on $Si/SiO_2/TiO_2/Pt$ from the BST–MEG sol resulted in a homogeneous and dense microstructures, whereas the BST thin films deposited from the BST–EGME sols resulted in a porous and non-uniform microstructures.

Acknowledgments

This work is supported by the National Nature Science Foundation of China under Grant no. u0837605.

References

[1] Somnath C. Roya, G.L. Sharma, M.C. Bhatnagara, R. Manchanda, Effect of pH on electrical and optical properties of sol–gel derived microcrystalline $Ba_{0.5}Sr_{0.5}TiO_3$ thin films, Applied Surface Science 236 (2004) 306–312.

[2] K.-T. Kim, C.–I. Kim, Structure and dielectric properties of Bi-doped $Ba_{0.6}Sr_{0.4}TiO_3$ thin films fabricated by sol–gel method, Microelectronic Engineering 66 (2003) 835–841.

[3] S.H. Xiao, J. Hu, H.J. Xu, W.F. Jiang, X.J. Li, The calculation of the optimum pH range for synthesizing BST nanopowders by sol–gel auto-combustion process, Journal of Sol-Gel Science and Technology 49 (2009) 166–169.

[4] H. Lu, J.S. Pan, X.F. Chen, Influence of annealing temperature on the band structure of sol–gel $Ba_{0.65}Sr_{0.35}TiO_3$ thin films on n-type Si(100), Applied Physics Letters 88 (2006) 132907.

[5] A. Veber, S. Kunej, R.C. Korosec, D. Suvorov, The effects of solvents on the formation of sol–gel-derived $Bi_{12}SiO_{20}$ thin films, Journal of the European Ceramic Society 30 (2010) 2475–2480.

[6] H.W. Chen, C.R. Yang, C.L. Fu, L. Zhao, Z.Q. Gao, The size effect of $Ba_{0.6}Sr_{0.4}TiO_3$ thin films on the ferroelectric properties, Applied Surface Science 252 (2006) 4171–4177.

[7] D. Wu, A.D. Li, X.B. Yin, Preparation of $Ba_{0.5}Sr_{0.5}TiO_3$ thin films by sol–gel method with rapid thermal annealing, Applied Surface Science 165 (2000) 309–314.

[8] Y.P. Ding, C.Y. Jin, Z.Y. Meng, Investigation on the amorphous–crystalline transition and microstructure of sol–gel derived $Ba_{1-x}Sr_x$-TiO_3 thin films, Materials Research Bulletin 35 (2000) 1187–1193.

[9] X.F. Chen, W.Q. Lu, W.G. Zhu, S.Y. Lim, Sheikh A. Akbar, Structural and thermal analyses on phase evolution of sol–gel (Ba,Sr)TiO_3 thin films, Surface and Coatings Technology 167 (2003) 203–206.

[10] Maria C. Gust, Neal D. Evans, Leslie A. Momoda, Martha L. Mecartney, In-situ transmission electron microscopy crystallization studies of sol–gel-derived barium titanate thin films, Journal of the American Ceramic Society 80 (1997) 2828–2836.

[11] W.H. Chen, B.Y. Ni, W.B. Wu, Effects of the sol concentration on the texture of $Pb_{0.3}Sr_{0.7}TiO_3$ thin films derived by sol–gel method, Journal of Electroceramics 21 (2008) 664–667.

[12] K.G. Kanade, B.B. Kale, R.C. Aiyer, B.K. Das, Thickness, Morphology and structure of sol–gel hybrid films: II—the role of the solvent, Materials Research Bulletin 41 (2006) 590–600.